Mass-imbalance effect on the cluster formation in a one-dimensional Fermi gas with coexistent s- and p-wave interactions

Yixin Guo (郭一昕)1,*

¹RIKEN Nishina Center for Accelerator-Based Science, Wako 351-0198, Japan (Dated: November 19, 2025)

We consider the mass-imbalance effect on the clustering in a one-dimensional two-component Fermi gas with coexistent even- and odd-wave interactions resulting in different configurations of clustering phases. We obtain the solutions of both stable two- and three-body cluster states with different mass ratios and configurations by solving the corresponding variational equations. We feature out phase diagrams consisting of the s- and p-wave pairing phases, and tripling phase with different configurations, in a plane of s- and p-wave pairing strengths. As for the in-vacuum case, the three-body clustering is always the lowest-lying phase. While for the in-medium case, the Cooper tripling phase dominates over the pairing phases when both s- and p-wave interactions are moderately strong. There is also a competition between different clustering configurations of three-body clustering.

I. INTRODUCTION

The investigation of superconductors and superfluids has been one of the frontiers in modern physics. It is indicated that the competition and the coexistence of various orders are worth being investigated [1–5], which have important applications in different fields such as condensed-matter and nuclear physics. However, to understand the microscopic mechanism of non-trivial states arising in the mass-imbalanced systems with coexistent orders is still one of the most challenging open questions.

It would be useful to study the mass-imbalance effect on multibody clustering in various systems. The Efimov state [6] has attracted lots of interest in ultracold atoms, nuclear physics, and so on. In the corresponding investigation, experimental evidence of Efimov physics has been reported in different mass-imbalanced ultracold atomic gas mixtures such as ⁴¹K-⁸⁷Rb [7] or ⁶Li-¹³³Cs [8] ones. The two-nucleon halo nuclei such as ¹¹Li (⁹Li core + 2 halo neutrons) is also regarded as an ideal candidate to experimentally detect the Efimov states [9]. So far, various possible superconductors with competing odd- and even-parity pairing channels have been experimentally realized in the mass-imbalanced systems, including UTe₂ [4, 10], UPt₃ [11], WTe₂ [12], and Sr₂RuO₄ [13, 14]. Moreover, in nuclear physics, there is also a novel state called hypernucleus consisting of at least one hyperon in addition to the normal nucleons [15]. It shows many interesting properties, such as that hypernuclei containing the lightest hyperon Λ (such as ${}^{7}_{\Lambda}$ Li) tend to be more tightly bound than normal nuclei [16]. The hypernuclei with small particle number would be useful for the preliminary studies.

The ultracold atomic gas is regarded as an ideal platform for investigating such non-trivial quantum many-body phenomena, due to its tunnable interactions

and densities [17, 18]. Both s- and p-wave interactions are tunable near the Feshbach resonance [18–24]. Consequently, it is interesting to realize the situation that Fermi superfluids with hybridized s- and p-wave pairings in cold atomic systems via overlapped Feshbach resonances [17, 25, 26]. In such a system, in addition to s- and p-wave Cooper pairings, the clustering associated with the Cooper instability may be extended to induce the bound states consisting of three particles or even more. In order to study such a many-body problem, the generalized Cooper problem has been further applied to cluster states such as three-body Cooper triples [5, 27– 32] and even four-body Cooper quartets [33–38]. On the other hand, with the help of specific geometry and trap potential, low dimensions and lattice structures can be achieved in cold-atomic systems [39–42]. Such low-dimensional systems in condensed-matter or nuclear physics have also attracted much attention [43–45].

In the previous work [5], we studied the degenerate two-component fermions with coexistent interspecies and intraspecies interactions, which lead to the Cooper instabilities towards the s- and p-wave Cooper pairs, and the Cooper triple with mass-balanced configuration. However, the mass imbalance is also worth being investigated, and the intraspecies interaction is not necessary limited to exist only within one component. In this work, we are going to figure out the properties in a system with both s- and p-wave interactions as shown in Fig. 1. The two- and three-body clusterings with different configurations are also anticipated. In Ref. [46], by activating the orbitals degree of freedom, the authors reported that the emergence of even-parity (s-wave) interaction in a spin-polarized fermionic ⁴⁰K gas besides the odd-wave (p-wave) interactions among identical fermions in each orbital. Based on that, present model setup might be achieved experimentally via fulfilling multiorbital structure with different components of atoms in the future.

In this paper, we investigate the fate of in-vacuum and in-medium two- and three-body correlations in a one-

^{*} yixin.guo@riken.jp

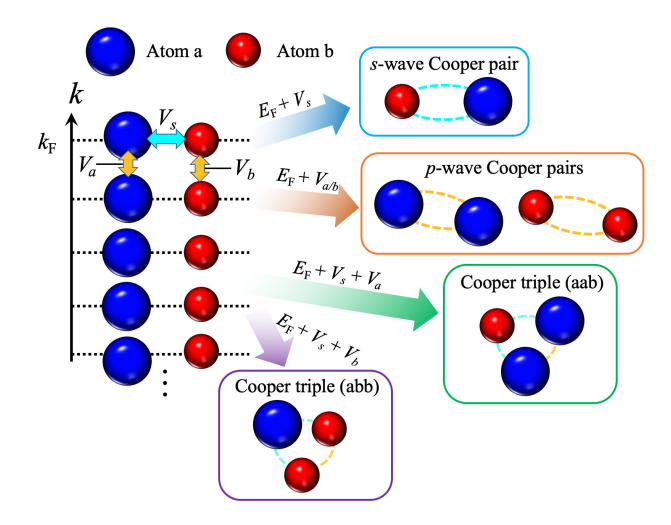


FIG. 1. Schematic figure representing our model. We consider the degenerate two-component mass-imbalanced fermions (states a and b occupying the levels with momentum k up to the Fermi momentum k_F) and the consequence of coexistent interspecies s-wave interaction V_s and intraspecies p-wave interactions V_i (acting on two identical fermions in the i=a,b state), which lead to the Cooper instabilities towards the s-and p-wave Cooper pairs, and the Cooper triples.

dimensional two-component Fermi gas with coexistent s-and p-wave interactions. Specific attention is paid to the mass imbalance and different configurations of clustering. In general, the mass of two components of fermions are adopted as different ones, and p-wave interactions among both kinds of atoms are taken into considerations. By solving the variational equations, we show the solutions of the stable clusters. We also figure out a phase diagram consisting of pairing and tripling states with different configurations.

This paper is organized as follows. The theoretical framework is presented in Sec. II, where we show the Hamiltonian for present system. We apply a variational approach for in-medium two- and three-body states on top of the Fermi sea to this model. In Sec. III A, we first discuss our numerical results for the in-vacuum bound states and the ground-state phase diagram. The results of in-medium case are shown in Sec. III B. Finally, a summary and perspectives will be given in Sec. IV. In the following, we take $\hbar=c=k_{\rm B}=1$. The system size is taken to be a unit.

II. THEORETICAL FRAMEWORK

In this work, we consider a one-dimensional massimbalanced two-component fermions with coexistent short-range interactions. The intraspecies odd-parity (p-wave) interactions among each kind of fermions are both taken into considerations. While as for the interspecies interaction, we assume the even-parity (s-wave) one is dominant and neglect the odd-parity (p-wave) interaction

one as the same as the previous work [5]. Consequently, the present system can be described by the following Hamiltonian as

$$H = K + V_s + V_a + V_b, \tag{1}$$

$$K = \sum_{k} \left(\xi_{k,a} a_k^{\dagger} a_k + \xi_{k,b} b_k^{\dagger} b_k \right), \tag{2}$$

$$V_a = \frac{U_a}{2} \sum_{p,p',a} pp' a^{\dagger}_{p+q/2} a^{\dagger}_{-p+q/2} a_{-p'+q/2} a_{p'+q/2}, \quad (3)$$

$$V_b = \frac{U_b}{2} \sum_{p,p',q} pp' b_{p+q/2}^{\dagger} b_{-p+q/2}^{\dagger} b_{-p+q/2} b_{-p'+q/2} b_{p'+q/2}, \qquad (4)$$

$$V_s = U_s \sum_{p,p',q} a^{\dagger}_{p+\frac{m_r}{m_b}q} b^{\dagger}_{-p+\frac{m_r}{m_a}q} b_{-p'+\frac{m_r}{m_a}q} a_{p'+\frac{m_r}{m_b}q}, \quad (5)$$

where $\xi_{k,i}=k^2/(2m_i)-\mu_i$ (i=a,b) in the kinetic term K is the single-particle energy with a momentum k, an atomic mass m_i , and chemical potential μ_i . Here the reduced mass reads $m_r=\frac{m_am_b}{m_a+m_b}$. Note that in general the cases with $m_a\neq m_b$ will be considered in this paper. In the generalized Cooper problems, we take $\mu_i=E_{{\rm F},i}$ where $E_{{\rm F},i}$ is the Fermi energy of species i. Due to the mass difference, there is a mismatch of the Fermi energy (or chemical potential) between two different kinds of fermions, namely, $\mu_a\neq \mu_b$. V_i represents the two-body p-wave interaction between two identical atoms i with a coupling constant U_i , and V_s corresponds to the two-body s-wave interaction with a coupling constant U_s . The contact couplings U_s and U_i can be renormalized by introducing the s-wave and p-wave scattering lengths as

$$U_s = -\frac{1}{m_r a_s},\tag{6}$$

and

$$\frac{m_i}{2a_p} = \frac{1}{U_i} + \sum_{p} \frac{p^2}{2\varepsilon_{p,i}} \tag{7}$$

with $\varepsilon_{p,i} = p^2/(2m_i)$, respectively. Here we assume the p-wave scattering lengths of two components are always tuned to be equal to each other. Incidentally, we are interested in an attractive s-wave interaction in this work, the positive s-wave scattering length $a_s > 0$ is taken.

As schematically shown in Fig. 1, with the mass imbalance and the p-wave interactions among both kinds of atoms, there are in total five phases of correlations expected to appear in the present system. In detail, as for the pairing states, we have s-wave pairing, p-wave pairing (aa configuration) and p-wave pairing (bb configuration). While for the tripling states, we have aab and abb configurations, respectively.

The trial wave functions for these in-medium two-and

three-body states are adopted as

$$|\Psi_{ab}\rangle = \sum_{k} \theta(|k| - k_{\rm F}) \Omega_{k}^{ab} a_{k}^{\dagger} b_{-k}^{\dagger} |\text{FS}\rangle$$
$$= \sum_{k}' \Omega_{k}^{ab} a_{k}^{\dagger} b_{-k}^{\dagger} |\text{FS}\rangle, \tag{8}$$

for s-wave pairing state [47],

$$|\Psi_{aa}\rangle = \sum_{k} \theta(|k| - k_{\rm F}) \Omega_{k}^{aa} a_{k}^{\dagger} a_{-k}^{\dagger} |FS\rangle$$
$$= \sum_{k}' \Omega_{k}^{aa} a_{k}^{\dagger} a_{-k}^{\dagger} |FS\rangle, \tag{9}$$

for p-wave pairing (aa configuration) state [31],

$$|\Psi_{bb}\rangle = \sum_{k} \theta(|k| - k_{\rm F}) \Omega_{k}^{bb} b_{k}^{\dagger} b_{-k}^{\dagger} |FS\rangle$$
$$= \sum_{k}' \Omega_{k}^{bb} b_{k}^{\dagger} b_{-k}^{\dagger} |FS\rangle, \tag{10}$$

for p-wave pairing (bb configuration) state,

$$|\Psi_{aab}\rangle = \sum_{p,q} \theta(|p+q/2| - k_{\rm F})\theta(|-p+q/2| - k_{\rm F})$$

$$\times \theta(|-q| - k_{\rm F})\Omega_{p,q}^{aab} a_{p+q/2}^{\dagger} a_{-p+q/2}^{\dagger} b_{-q}^{\dagger} |\text{FS}\rangle$$

$$= \sum_{p,q}' \Omega_{p,q}^{aab} a_{p+q/2}^{\dagger} a_{-p+q/2}^{\dagger} b_{-q}^{\dagger} |\text{FS}\rangle,$$
(11)

for tripling (aab configuration) state [5], and

$$|\Psi_{abb}\rangle = \sum_{p,q} \theta(|p+q/2| - k_{\rm F})\theta(|-p+q/2| - k_{\rm F})$$

$$\times \theta(|-q| - k_{\rm F})\Omega_{p,q}^{abb}a_{-q}^{\dagger}b_{p+q/2}^{\dagger}b_{-p+q/2}^{\dagger}|{\rm FS}\rangle$$

$$= \sum_{p,q}' \Omega_{p,q}^{abb}a_{-q}^{\dagger}b_{p+q/2}^{\dagger}b_{-p+q/2}^{\dagger}|{\rm FS}\rangle,$$
(12)

for tripling (abb configuration) state, respectively. In the above trial wave functions, $\Omega^{mn\cdots}_{q_1,q_2,\cdots}$ denotes the variational parameter for the state with $mn\cdots$ configuration and a set of momenta q_1,q_2,\cdots , and $|\text{FS}\rangle$ represents the Fermi sea. From the parity and symmetry, it is easy to find $\Omega^{iij}_{p,q} = -\Omega^{iij}_{-p,q}$ and $\Omega^{iij}_{p,q} = \Omega^{iij}_{p,-q}$ (i,j=a,b and $i\neq j$) for Cooper triple phases. In addition, here $\sum_{i=1}^{n}$ is adopted

to denote the the momentum summation restricted by the Fermi surface for convenience. The step functions associated with the Fermi surface will be recovered when we numerically evaluate the momentum summation. By minimizing the in-medium two- and three-body ground-state energies based on the variational principle, the variational parameter $\Omega_{q_1,q_2,\dots}^{mn\cdots}$ will be determined correspondingly.

Calculating the expectation values of Hamiltonian associated with each trial wave function $\langle \Psi_{mn}...|H|\Psi_{mn}...\rangle$, and then applying the variational principle, we arrive that

$$\frac{\delta}{\delta\Omega_{q_1,q_2,\dots}^{mn\dots}} \langle \Psi_{mn\dots} | (H - E_{\alpha}^{mn\dots}) | \Psi_{mn\dots} \rangle = 0, \quad (13)$$

where $E_{\alpha}^{mn\cdots}$ ($\alpha=2,3$) is the ground-state energy of a Cooper cluster with $mn\cdots$ configuration. As a result, the in-medium variational equations read

$$1 + U_s \sum_{q}^{\prime} \frac{1}{\xi_{q,a} + \xi_{q,b} - E_{2,s}} = 0, \tag{14}$$

for the s-wave pairing [47],

$$1 + U_i \sum_{p}' \frac{p^2}{\xi_{p,i} + \xi_{-p,i} - E_{2,p}^{ii}} = 0,$$
 (15)

for p-wave pairing (ii configuration) [31],

$$(\xi_{p+q/2,a} + \xi_{-p+q/2,a} + \xi_{-q,b} - E_3^{aab})\Omega_{p,q}^{aab} + p\Gamma_p^{aab}(q) + \Gamma_s^{aab}(p-q/2) - \Gamma_s^{aab}(-p-q/2) = 0,$$
 (16)

for tripling (aab configuration) [5], and

$$(\xi_{-q,a} + \xi_{p+q/2,b} + \xi_{-p+q/2,b} - E_3^{abb})\Omega_{p,q}^{abb} + p\Gamma_p^{abb}(q) + \Gamma_s^{abb}(p - q/2) - \Gamma_s^{abb}(-p - q/2) = 0,$$
(17)

for tripling (abb configuration), respectively. To simplify the ensuing expressions, in the above variational equations we introduce

$$\Gamma_{p}^{iij}(q) = U_{i} \sum_{p'}' p' \Omega_{p',q}^{iij}, \quad \Gamma_{s}^{iij}(k) = U_{s} \sum_{q'}' \Omega_{k+q'/2,q'}^{iij},$$
(18)

with i, j = a, b and $i \neq j$. We also figure out that

$$\Gamma_p^{iij}(q) = \Gamma_p^{iij}(-q), \quad \Gamma_s^{iij}(k) = -\Gamma_s^{iij}(-k). \tag{19}$$

Correspondingly, the in-medium three-body equations for $\Gamma_p^{iij}(q)$ and $\Gamma_s^{iij}(k)$ reads

$$\Gamma_p^{iij}(q) \left[1 + U_i \sum_{p}' \frac{p^2}{\xi_{p+q/2,i} + \xi_{-p+q/2,i} + \xi_{-q,j} - E_3^{iij}} \right]
= -U_i \sum_{p}' p \frac{\Gamma_s^{iij}(p - q/2) - \Gamma_s^{iij}(-p - q/2)}{\xi_{p+q/2,i} + \xi_{-p+q/2,i} + \xi_{-q,j} - E_3^{iij}},$$
(20)

and

$$\Gamma_s^{iij}(k) \left[1 + U_s \sum_{q}' \frac{1}{\xi_{k+q,i} + \xi_{-k,i} + \xi_{-q,j} - E_3^{iij}} \right]
= -U_s \sum_{q}' \frac{(k+q/2)\Gamma_p^{iij}(q) - \Gamma_s^{iij}(-k-q)}{\xi_{k+q,i} + \xi_{-k,i} + \xi_{-q,j} - E_3^{iij}},$$
(21)

respectively.

Before discussing the numerical demonstrations in detail, we note that present variational approach is able to describe the BCS-BEC crossover and its three-body counterpart qualitatively [48]. The variational wave functions for calculating the energies of Cooper clusters can well depict both the Cooper clustering in the weak-coupling BCS limit and the tightly bound state formation in the strong-coupling BEC limit in a unified manner.

III. RESULTS AND DISCUSSION

A. In-vaccum case

In the absence of the Fermi sea, namely, by taking the reference state as the vacuum $|0\rangle$ instead of the Fermi sea $|FS\rangle$, we first investigate the in-vacuum two- and three-body clustering in present mass-imbalanced two-component Fermi gas.

In Fig. 2, by taking the mass ratio $m_a = 2m_b$ as a typical example, we plot in-vacuum clustering energies as functions of scattering lengths. As for the in-vacuum two-body energies shown in Figs. 2(a) and (b), the s(p)-wave pairing one monotonically decreases with the increase of s(p)-wave interaction strengths. From Fig. 2(b), it is seen that the in-vacuum two-body pairing with aa configuration is always suppressed by the one with bb configuration. It is due to the mass difference, where the pairing consisting of lighter atoms is more tightly bound at a fixed interaction strength. Such a tendency can be qualified from Eq. (15). One has

$$\frac{E_{2,p}^{ii}}{E_{\Lambda}} \propto \frac{m_r}{m_i} \tag{22}$$

in the reference scale of $E_{\Lambda} = \Lambda^2/(2m_r)$, where Λ denotes the momentum cutoff adopted in the practical calculations. It naturally indicates p-wave bb pairing is more tightly bound than the aa configuration.

In Fig. 2(c), by fixing $1/(\Lambda a_s) \times 10 = 2.7$, the invacuum three-body energies negatively become larger with stronger p-wave interaction. Among the in-vacuum three-body clusters, the aab configuration is dominant in the regime $1/(\Lambda a_p) \times 10 \lesssim 0.25$, while the abb one becomes stabler when $1/(\Lambda a_p) \times 10$ exceeds 0.25. In other words, there is a competition between two different configurations of in-vacuum three-body clusters, which also results from the mass difference.

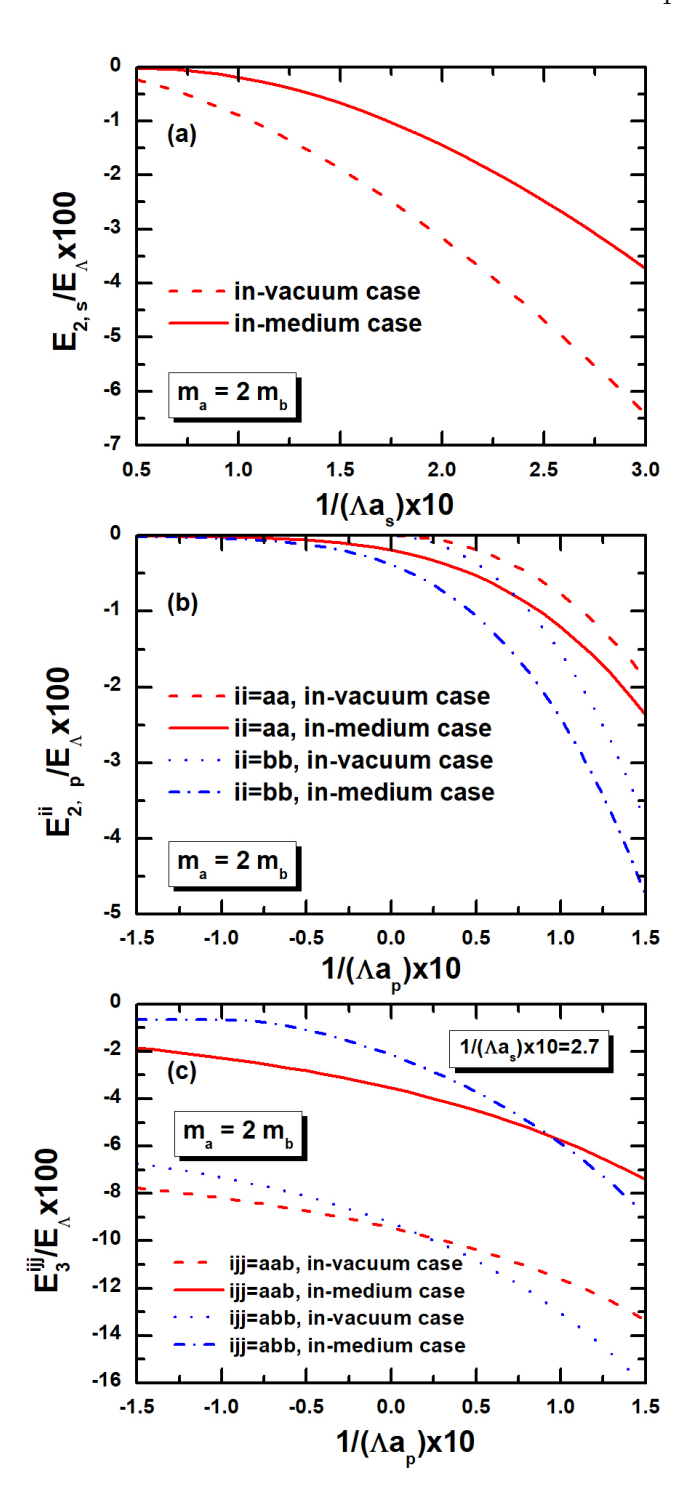


FIG. 2. (a). In-vacuum and in-medium s-wave pairing energies as functions of s-wave scattering length. (b). In-vacuum and in-medium p-wave pairing energies with different configurations as functions of p-wave scattering length. (c). In-vacuum and in-medium three-body energies with different configurations as functions of p-wave scattering length at fixed s-wave interaction strength as $1/(\Lambda a_s) \times 10 = 2.7$ with Λ the momentum cutoff. In all panels, mass ratio is fixed as $m_a/m_b = 2$, and the reference energy scale is $E_{\Lambda} = \Lambda^2/(2m_r)$.

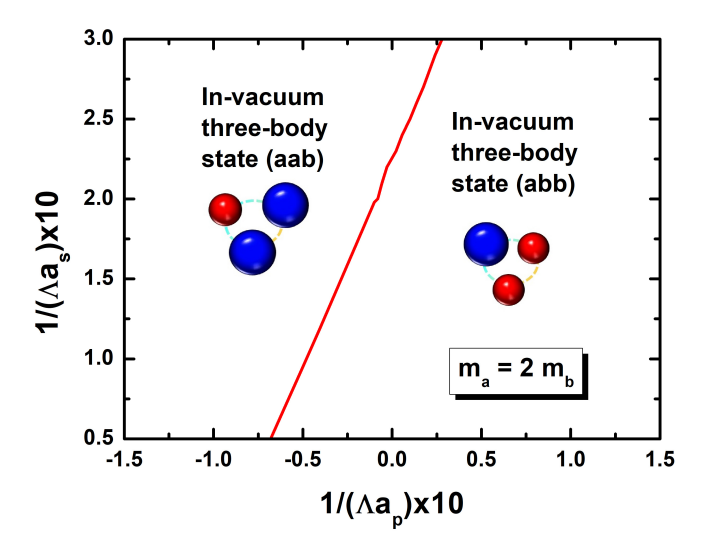


FIG. 3. In-vacuum phase diagram in the plane of $1/(\Lambda a_s)$ and $1/(\Lambda a_p)$. The mass ratio is taken as $m_a = 2m_b$.

We feature out the in-vacuum phase diagram in the plane of $1/(\Lambda a_s)$ and $1/(\Lambda a_p)$ as shown in Fig. 3. The in-vacuum phase diagram gives the lowest-lying phase among all the five configurations of two- or three-body clusters discussed in this work. The mass ratio is taken as $m_a = 2m_b$. It is seen that in the interaction regime concerned in this paper, $|E_3| > |E_2|$ always holds regardless of specific two- and three-body configurations in the in-vacuum case. Moreover, at a fixed s-wave interaction, with the increase of p-wave interaction, the lowest-lying phase changes from the three-body states with aab configuration to those with abb configuration. In other words, the in-vacuum three-body states with abb configuration become dominant in the regime with stronger p-wave interaction. It is because the increase of p-wave attraction induces larger enhancement for bbpairings with smaller mass compared to aa ones.

B. In-medium case

To see effects from the mass imbalance to the inmedium three-body ground-state energy, in Fig. 4, we plot the contour plot of in-medium three-body energy E_3^{aab}/E_0 in a plane of mass m_a/m_0 and m_b/m_0 . For comparison, the mass m_0 and energy $E_0 = k_{\rm F}^2/(2m_0)$ are taken as the reference scales. The interaction strengths are fixed at $1/(k_{\rm F}a_s) = 1/(k_{\rm F}a_p) = 1.5$. The momentum cutoff Λ is taken as $10k_{\rm F}$. In the present two-component Fermi gas, as for one species of atom with a fixed mass, if we gradually enlarge the mass of another one, the absolute value of E_3^{aab} monotonically decreases. Such a qualitative behavior is a result of fixed interaction strengths. Moreover, it is also seen that a smaller reduced mass $m_r = m_a m_b/(m_a + m_b)$ gives an negatively larger E_3^{aab} in Fig. 4.

In order to see the competition between the in-medium

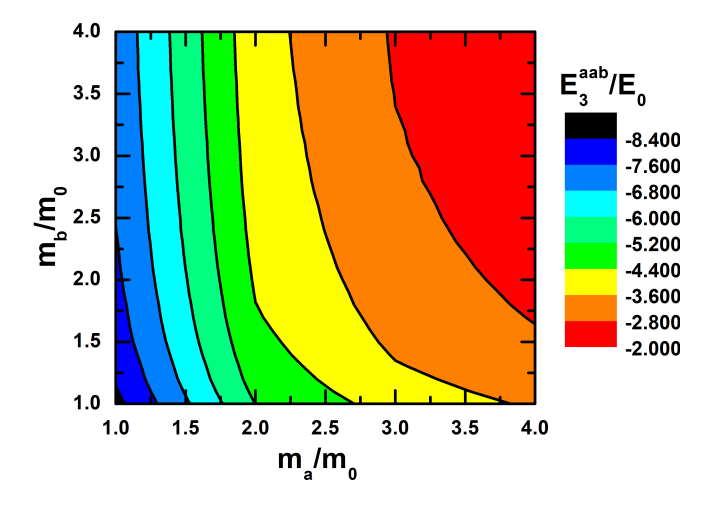


FIG. 4. Contour plot of in-medium three-body energy E_3^{aab}/E_0 in a plane of mass m_a/m_0 and m_b/m_0 . The mass m_0 and energy $E_0 = k_{\rm F}^2/(2m_0)$ are taken as the reference scales. The interaction strengths are fixed at $1/(k_{\rm F}a_s) = 1/(k_{\rm F}a_p) = 1.5$. The momentum cutoff is taken as $10k_{\rm F}$.

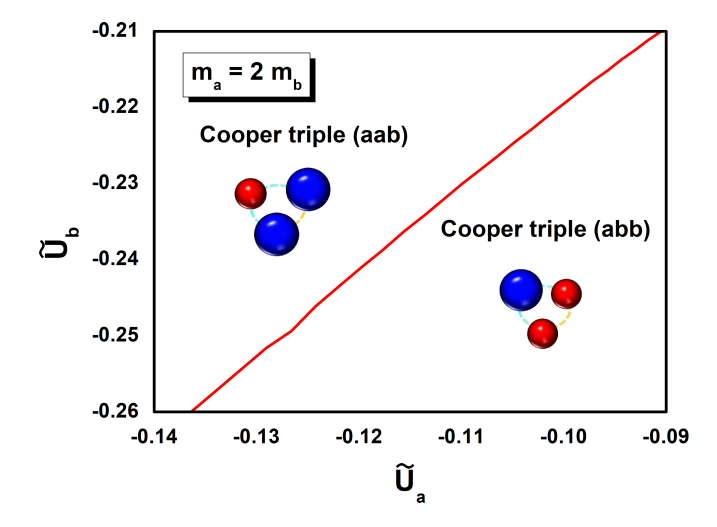


FIG. 5. Lower-lying excited state of Cooper triple phases with different configurations in a plane of two-body p-wave interaction strengths. The mass ratio is taken as $m_a = 2m_b$, and the momentum cutoffs are taken as $\Lambda/k_{\rm F} = 10$.

three-body correlations with different configurations in the present system, by fixing the mass ratio as $m_a=2m_b$, we plot the lower-lying excited state of Cooper triple phases with different configurations in a plane of two-body p-wave interaction strengths in Fig. 5. Here the dimensionless p-wave coupling strengths are defined as $\tilde{U}_i=2m_rk_FU_i$. In this paper, we consider the attractive two-body p-wave interactions, which indicates that a larger absolute value of \tilde{U}_i represents a stronger attraction. At a fixed p-wave interaction strength \tilde{U}_a among atoms a, when the p-wave interaction strength \tilde{U}_b among atoms b increases to a certain value, the dominant (lower-lying) Cooper triple state changes from the aab

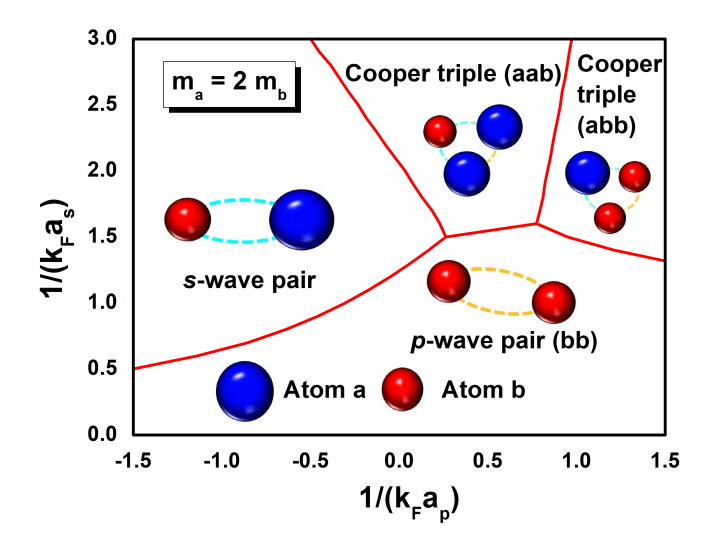


FIG. 6. Phase diagram of s-wave pairing ($|E_{2,s}| > |E_{2,p}^{ii}|$, $|E_{3}^{iij}|$), p-wave pairings ($|E_{2,p}^{ii}| > |E_{2,s}|$, $|E_{3}^{iij}|$), and Cooper tripling ($|E_{3}^{iij}| > |E_{2,s}|$, $|E_{2,p}^{ii}|$) in the plane of $1/(k_{\rm F}a_s)$ and $1/(k_{\rm F}a_p)$ (i,j=a,b). The mass ratio is taken as $m_a=2m_b$, and the momentum cutoffs are taken as $\Lambda/k_{\rm F}=10$.

configuration to the abb one. The similar behavior holds for a fixed p-wave interaction strength \tilde{U}_b among atoms b. The competition between two different configurations of Cooper triples is similar to the in-vacuum case shown in Fig. 3, which results from the mass difference.

At last, by taking the mass ratio as $m_a = 2m_b$, we summarize the ground-state phase diagram of sand p-wave Cooper pairing states, and the Cooper triple states with different configurations in Fig. 6. The boundary lines between different kinds of Cooper clustering phases are determined in such a way that the one between tripling (iii configuration) and s-wave pairing, that between tripling (iij configuration) and pwave pairing (ii configuration), and that between s- and p-wave pairing (ii configuration) are given by $E_3^{iij} = E_{2,s}$, $E_3^{iij} = E_{2,p}^{iii}$, and $E_{2,s} = E_{2,p}^{ii}$, respectively. The range of scattering parameters in Fig. 6 [0.5 $\leq 1/(k_{\rm F}a_s) \leq 3$ and $-1.5 \leq 1/(k_{\rm F}a_p) \leq 1.5$] are adopted as same one in Ref. [5], which are also similar values were realized in a recent experimental work [46]. Such a phase diagram captures interesting features associated with competing s- and p-wave pairings and moreover tripling. In order to investigate the physics behind more, we also plot in-medium clustering energies as functions of scattering lengths in Fig. 2. From Fig. 2, it is shown that the presence of the Fermi sea reshapes the formation of pairing and three-body states. Moreover, by comparing Fig. 2(a) [or (b)] and (c), the presence of Fermi surface affects three-body energies much more than pairing ones. Consequently, it is seen that when s- or p-wave interaction strength is comparably weak, the pairing phases survive, which is different to the in-vacuum case. As for the pairing

states, the p-wave pair (aa configuration) phase is always suppressed due to the mismatch of Fermi energies between atoms a and b, where the Cooper instability among heavier atoms becomes weaker. As for the tripling states, the Cooper triple (aab configuration) phase survives due to the coexistence of both s- and pwave interactions, where the effect from the mismatch of Fermi energies is partially offset by the inclusion of s-wave attraction. In the meanwhile, similar to the invacuum case shown in Fig. 3, there is a competition between Cooper triple (aab configuration) phase and Cooper triple (abb configuration) phase. On the one hand, we have numerically checked that the qualitative behaviors of the boundary line between s-wave pair phase and Cooper triple (aab configuration) phase, and that between Cooper triple (aab configuration) phase and Cooper triple (abb configuration) phase are unchanged even up to a extremely large s-wave interaction strength [such as $1/(k_{\rm F}a_s) = 10.0$]. It indicates that the competition between different configurations of Cooper triple phases may also result from the difference of scatterings between s-wave dimer (ab configuration) and each component of atoms. In the meanwhile, at a fixed s-wave interaction strength, bb configuration with a smaller mass also becomes more tightly bound than the aa configuration as the p-wave scattering length increases due to the mismatch of Fermi energy between atoms a and b. In other words, the Cooper triple (abb configuration) is expected to be stabler than the Cooper triple (aab configuration) in the stronger p-wave interaction regime. As for the cutoff dependence, we have numerically checked that while the regime of Cooper triple phases gets enlarged with larger momentum cutoff Λ , the boundaries between different kinds of pairings remain robust. Such a cutoff dependenc is also similar to that in the previous work [5]. Even though the specific value of momentum cutoff in the practical calculations is needed to compare our results with the experiments, our phase diagram would be useful to understand the qualitative features of hybridized s- and p-wave interacting systems with mass imbalance and different configurations of clustering.

IV. SUMMARY AND PERSPECTIVES

As a step further of previous work [5], in this paper we have investigated the mass imbalance and different kinds of clustering configurations in the system with the coexistence s- and p-wave interactions. We have investigated both the in-vacuum and in-medium two- and three-body correlations in the mass-imbalanced two-component Fermi gas. The solutions of in total five kinds of stable in-medium two- and three-body cluster states have been found in this system by solving the variational equations. By taking a certain mass ratio between two components of fermions, we have featured out a ground-state phase diagram consisting of s- and p-wave

pairing states, and the Cooper triple states with different configurations in a plane of s- and p-wave scattering lengths.

With the inclusion of mass imbalance and different clustering configurations, our work would be useful for the deeper understanding and better understanding of the nontrivial states arising in the systems with the coexistence of both even-parity (s-wave) and odd-parity (p-wave) interactions. Present results would also be useful for the further investigation of unconventional superfluids and superconductors. For the future perspectives, it is also interesting to see how similar in-

medium correlations may arise in other systems, such as condensed-matter or nuclear ones. For instance, our present model setup may be applied to the investigations of hypernuclei with the lightest hyperon Λ [15].

ACKNOWLEDGMENTS

The author thanks Hiroyuki Tajima for useful discussions. Y.G. was supported by RIKEN Special Postdoctoral Researchers Program.

- [1] S. Yasui, D. Inotani, and M. Nitta, Coexistence phase of ¹S₀ and ³P₂ superfluids in neutron stars, Phys. Rev. C 101, 055806 (2020).
- [2] F. M. Marqués and J. Carbonell, The quest for light multineutron systems, The European Physical Journal A 57, 1 (2021).
- [3] M. Duer, T. Aumann, R. Gernhäuser, V. Panin, S. Paschalis, D. Rossi, N. Achouri, D. Ahn, H. Baba, C. Bertulani, et al., Observation of a correlated free fourneutron system, Nature 606, 678 (2022).
- [4] S. Kanasugi and Y. Yanase, Anapole superconductivity from PT-symmetric mixed-parity interband pairing, Commun. Phys. 5, 1 (2022).
- [5] Y. Guo and H. Tajima, Competition between pairing and tripling in one-dimensional fermions with coexistent s- and p-wave interactions, Phys. Rev. B 107, 024511 (2023).
- [6] V. Efimov, Energy levels arising from resonant two-body forces in a three-body system, Phys. Lett. B 33, 563 (1970).
- [7] G. Barontini, C. Weber, F. Rabatti, J. Catani, G. Thalhammer, M. Inguscio, and F. Minardi, Observation of heteronuclear atomic efimov resonances, Phys. Rev. Lett. 103, 043201 (2009).
- [8] R. Pires, J. Ulmanis, S. Häfner, M. Repp, A. Arias, E. D. Kuhnle, and M. Weidemüller, Observation of efimov resonances in a mixture with extreme mass imbalance, Phys. Rev. Lett. 112, 250404 (2014).
- [9] D. V. Fedorov, A. S. Jensen, and K. Riisager, Efimov states in halo nuclei, Phys. Rev. Lett. 73, 2817 (1994).
- [10] L. Jiao, S. Howard, S. Ran, Z. Wang, J. O. Rodriguez, M. Sigrist, Z. Wang, N. P. Butch, and V. Madhavan, Chiral superconductivity in heavy-fermion metal ute₂, Nature 579, 523 (2020).
- [11] J. Sauls, The order parameter for the superconducting phases of UPt₃, Adv. Phys. 43, 113 (1994), NoStop
- [12] Y. Jia, P. Wang, C.-L. Chiu, Z. Song, G. Yu, B. JÀck, S. Lei, S. Klemenz, F. A. Cevallos, M. Onyszczak, N. Fishchenko, X. Liu, G. Farahi, F. Xie, Y. Xu, K. Watanabe, T. Taniguchi, B. A. Bernevig, R. J. Cava, L. M. Schoop, A. Yazdani, and S. Wu, Evidence for a monolayer excitonic insulator, Nat. Phys. 18, 87 (2022).
- [13] A. P. Mackenzie and Y. Maeno, The superconductivity of Sr₂RuO₄ and the physics of spin-triplet pairing, Rev. Mod. Phys. **75**, 657 (2003).
- [14] K. Kinjo, M. Manago, S. Kitagawa, Z. Q. Mao,

- S. Yonezawa, Y. Maeno, and K. Ishida, Superconducting spin smecticity evidencing the Fulde-Ferrell-Larkin-Ovchinnikov state in Sr₂RuO₄, Science **376**, 397 (2022).
- [15] M. Danysz and J. Pniewski, Delayed disintegration of a heavy nuclear fragment: I, The London, Edinburgh, and Dublin Philosophical Magazine and Journal of Science 44, 348 (1953).
- [16] K. Tanida, H. Tamura, D. Abe, H. Akikawa, K. Araki, H. Bhang, T. Endo, Y. Fujii, T. Fukuda, O. Hashimoto, K. Imai, H. Hotchi, Y. Kakiguchi, J. H. Kim, Y. D. Kim, T. Miyoshi, T. Murakami, T. Nagae, H. Noumi, H. Outa, K. Ozawa, T. Saito, J. Sasao, Y. Sato, S. Satoh, R. I. Sawafta, M. Sekimoto, T. Takahashi, L. Tang, H. H. Xia, S. H. Zhou, and L. H. Zhu, Measurement of the B(E2) of ⁷/_ALi and shrinkage of the hypernuclear size, Phys. Rev. Lett. 86, 1982 (2001).
- [17] C. Chin, R. Grimm, P. Julienne, and E. Tiesinga, Feshbach resonances in ultracold gases, Rev. Mod. Phys. 82, 1225 (2010).
- [18] Y. Ohashi, H. Tajima, and P. van Wyk, Bcsâbec crossover in cold atomic and in nuclear systems, Prog. Part. Nucl. Phys. 111, 103739 (2020).
- [19] C. Ticknor, C. A. Regal, D. S. Jin, and J. L. Bohn, Multiplet structure of feshbach resonances in nonzero partial waves, Phys. Rev. A 69, 042712 (2004).
- [20] V. Gurarie, L. Radzihovsky, and A. V. Andreev, Quantum phase transitions across a p-wave feshbach resonance, Phys. Rev. Lett. 94, 230403 (2005).
- [21] C. H. Schunck, M. W. Zwierlein, C. A. Stan, S. M. F. Raupach, W. Ketterle, A. Simoni, E. Tiesinga, C. J. Williams, and P. S. Julienne, Feshbach resonances in fermionic ⁶Li, Phys. Rev. A 71, 045601 (2005).
- [22] Y. Inada, M. Horikoshi, S. Nakajima, M. Kuwata-Gonokami, M. Ueda, and T. Mukaiyama, Collisional properties of p-wave feshbach molecules, Phys. Rev. Lett. 101, 100401 (2008).
- [23] T. Nakasuji, J. Yoshida, and T. Mukaiyama, Experimental determination of p-wave scattering parameters in ultracold 6 Li atoms, Phys. Rev. A 88, 012710 (2013).
- [24] G. C. Strinati, P. Pieri, G. Röpke, P. Schuck, and M. Urban, The BCS-BEC crossover: From ultra-cold Fermi gases to nuclear systems, Phys. Rep. 738, 1 (2018), the BCS-BEC crossover: From ultra-cold Fermi gases to nuclear systems.
- [25] C. A. Regal, C. Ticknor, J. L. Bohn, and D. S. Jin, Tuning p-wave interactions in an ultracold fermi gas of

- atoms, Phys. Rev. Lett. 90, 053201 (2003).
- [26] L. Zhou, W. Yi, and X. Cui, Fermion superfluid with hybridized s-and p-wave pairings, Science China: Physics, Mechanics & Astronomy 60, 1 (2017).
- [27] P. Niemann and H.-W. Hammer, Pauli-blocking effects and cooper triples in three-component fermi gases, Phys. Rev. A 86, 013628 (2012).
- [28] T. Kirk and M. M. Parish, Three-body correlations in a two-dimensional su(3) fermi gas, Phys. Rev. A 96, 053614 (2017).
- [29] H. Tajima, S. Tsutsui, T. M. Doi, and K. Iida, Three-body crossover from a Cooper triple to a bound trimer state in three-component Fermi gases near a triatomic resonance, Phys. Rev. A 104, 053328 (2021).
- [30] H. Tajima, S. Tsutsui, T. M. Doi, and K. Iida, Cooper triples in attractive three-component fermions: Implication for hadron-quark crossover, Phys. Rev. Research 4, L012021 (2022).
- [31] Y. Guo and H. Tajima, Stability against three-body clustering in one-dimensional spinless p-wave fermions, Phys. Rev. A 106, 043310 (2022).
- [32] Y. Guo and H. Tajima, Cooper pairing and tripling in one-dimensional spinless fermions with attractive twoand three-body forces, Phys. Rev. A 108, 043303 (2023).
- [33] G. Röpke, A. Schnell, P. Schuck, and P. Nozières, Fourparticle condensate in strongly coupled fermion systems, Phys. Rev. Lett. 80, 3177 (1998).
- [34] N. Sandulescu, D. Negrea, J. Dukelsky, and C. W. Johnson, Quartet condensation and isovector pairing correlations in N=Z nuclei, Phys. Rev. C **85**, 061303 (2012).
- [35] V. Baran and D. Delion, A quartet BCS-like theory, Phys. Lett. B 805, 135462 (2020).
- [36] Y. Guo, H. Tajima, and H. Liang, Cooper quartet correlations in infinite symmetric nuclear matter, Phys. Rev. C 105, 024317 (2022).
- [37] Y. Guo, H. Tajima, and H. Liang, Biexciton-like quartet condensates in an electron-hole liquid, Phys. Rev. Research 4, 023152 (2022).

- [38] Y. Guo, T. Naito, H. Tajima, and H. Liang, Quartet correlations near the surface of N=Z nuclei, Phys. Rev. C **112**, 024310 (2025).
- [39] I. Bloch, J. Dalibard, and W. Zwerger, Many-body physics with ultracold gases, Rev. Mod. Phys. 80, 885 (2008).
- [40] H. Moritz, T. Stöferle, K. Günter, M. Köhl, and T. Esslinger, Confinement induced molecules in a 1d fermi gas, Phys. Rev. Lett. 94, 210401 (2005).
- [41] Y.-A. Liao, A. S. C. Rittner, T. Paprotta, W. Li, G. B. Partridge, R. G. Hulet, S. K. Baur, and E. J. Mueller, Spin-imbalance in a one-dimensional Fermi gas, Nature 467, 567 (2010).
- [42] T. Sowiński and M. Á. García-March, One-dimensional mixtures of several ultracold atoms: a review, Rep. Prog. Phys. 82, 104401 (2019).
- [43] C. Alexandrou, J. Myczkowski, and J. W. Negele, Comparison of mean-field and exact monte carlo solutions of a one-dimensional nuclear model, Phys. Rev. C 39, 1076 (1989).
- [44] K. Hagino, A. Vitturi, F. Pérez-Bernal, and H. Sagawa, Two-neutron halo nuclei in one dimension: dineutron correlation and breakup reaction, Journal of Physics G: Nuclear and Particle Physics 38, 015105 (2010).
- [45] F. Altomare and A. M. Chang, One-dimensional superconductivity in nanowires (John Wiley & Sons, 2013).
- [46] K. G. Jackson, C. J. Dale, J. Maki, K. G. S. Xie, B. A. Olsen, D. J. M. Ahmed-Braun, S. Zhang, and J. H. Thywissen, Emergent s-wave interactions between identical fermions in quasi-one-dimensional geometries, Phys. Rev. X 13, 021013 (2023).
- [47] Y. Ohashi, H. Tajima, and P. van Wyk, BCS-BEC crossover in cold atomic and in nuclear systems, Prog. Part. and Nucl. Phys. 111, 103739 (2020).
- [48] H. Tajima, S. Tsutsui, T. M. Doi, and K. Iida, Unitary p-wave Fermi gas in one dimension, Phys. Rev. A 104, 023319 (2021).